

An Analysis of the Inverse Kinematics for a 5-DOF Manipulator

De Xu^{*†‡}, Carlos A. Acosta Calderon, John Q. Gan, Huosheng Hu

[†]Department of Computer Science, University of Essex, Colchester CO4 3SQ, UK

Min Tan

[‡]The Key Laboratory of Complex System and Intelligence Science, Institute of Automation, Chinese Academy of Sciences, Beijing 100080, China

Abstract: This paper proposes an analytical solution for a 5-DOF manipulator to follow a given trajectory while keeping the orientation of one axis in the end-effector frame. The forward kinematics and inverse kinematics for a 5-DOF manipulator are analyzed systemically. The singular problem is discussed after the forward kinematics is provided. For any given reachable position and orientation of the end-effector, the derived inverse kinematics will provide an accurate solution. In other words, there exists no singular problem for the 5-DOF manipulator, which has wide application areas such as welding, spraying, and painting. Experiment results verify the effectiveness of the methods developed in this paper.

Keywords: Inverse kinematics, modeling and control, 5-DOF manipulator.

1 Introduction

Analytical techniques to deal with inverse kinematics have been well developed for manipulators with 6 degrees of freedom (DOF), especially after the work of Manocha and Canny^[1]. However, the deficiency of degrees of freedom makes the control of manipulators with less than 6-DOF very difficult when following a given trajectory with a desired final pose. A large number of unreachable positions and orientations which exist in the working space for an end-effector often result in no analytical solutions for the inverse kinematics^[2], although various artificial intelligence methods have been proposed for redundant and constrained manipulators^[3~5]. Recently, an analytical solution to the inverse kinematics of a 5-DOF Pioneer robotic arm (PArm) was developed at Essex^[2]. It works very well for any reachable position and orientation of the end-effector, and can provide very good approximate solutions for over 99% of situations that cannot be exactly reached.

As we know, it is impossible in most cases to completely satisfy the desired position and orientation of an end-effector with 6-DOF using a 5-DOF manipula-

tor. If any DOF of the end-effector is not maintained, then the desired position and orientation of the end-effector is reduced to 5-DOF. Obviously, analytical solutions for inverse kinematics exist in this case, and methods for dealing with them should be different depending on which DOF is not satisfied. In practice however, it is quite reasonable to satisfy the orientation defined by one coordinate vector only and the three-dimensional position of the end-effector. For example, when the manipulator is used for welding, the direction of the weld gun and position of its tip should match desired values. If the manipulator is mounted on a mobile robot, i.e. it can move with a mobile robot and serve as a mobile manipulator^[6,7], to keep the position of the end-effector free in the moving direction of the mobile robot is reasonable. These two typical cases in which the total number of DOF to be controlled is five are selected as examples to analyze the inverse kinematics of the PArm in this paper.

The rest of this paper is organized as follows. Section 2 presents the robotic arm platform and coordinate frame assignment. Forward kinematics analysis is introduced in Section 3. Section 4 presents the inverse kinematics analysis for a general case, and criteria for determining whether solutions for five joint angles exist. Solutions for two special cases concerned with a 5-DOF manipulator are derived in Section 5. Section 6 provides experiment results to show the feasibility of the proposed solution. Finally, the paper is concluded in Section 7.

Manuscript received June 4, 2005; revised December 12, 2005.

This work was supported by the National High Technology Research and Development Program of China (No. 2002AA422160), and the National Key Fundamental Research and Development Project of China (973, No.2002CB312200)

*Corresponding author. *E-mail address:* sdxude@yahoo.com

2 Coordinate frames for the PArm

The PArm is an accessory for the family of *Pioneer Mobile Robots*, as shown in Fig.1. It is a 5-DOF manipulator driven by six open-loop servomotors and has a gripper as an end-effector. The gripper has foamed fingers for firm grasping and manipulation of objects as large as a soda can and as heavy as 150 grams throughout the arm's envelope of operation^[8].

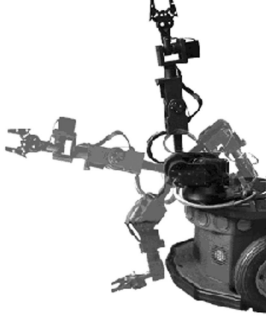


Fig.1 The PArm 5-DOF manipulator^[8]

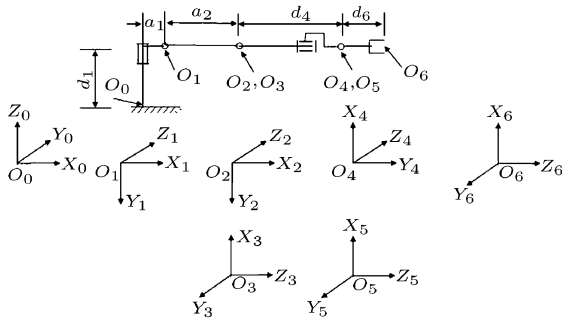


Fig.2 Coordinate frames for the PArm

Coordinate frames for the PArm are assigned as shown in Fig.2. They are established using the principles of the Denavit-Hartenberg (D-H) convention. Frame O_5 is an auxiliary frame attached to the end-effector at the place of joint 5, whose coordinate directions are the same as O_6 . Using the auxiliary frame O_5 to maintain consistency in the orientation for the last link of the manipulator keeps frames O_0 to O_5 in the same plane and this allows us to apply the geometric projection method to the derivation of the inverse kinematics.

3 Forward kinematics for the PArm

3.1 Forward kinematics

The forward kinematics is a set of equations that calculates the position and orientation of the end-effector in terms of given joint angles. This set of equations is generated by using the D-H parameters obtained from the frame assignment. The parameters for the PArm are listed in Table 1, where θ_i represents rotation about the Z -axis, α_i rotation about the X -axis, d_i transition along the Z -axis, and a_i transition along the X -axis.

Table 1 The D-H parameters of the PArm

Frame	θ_i	$d_i(mm)$	$a_i(mm)$	$\alpha_i(\text{degree})$
$O_0 - O_1$	θ_1	$d_1 = 120$	$a_1 = 68.75$	-90
$O_1 - O_2$	θ_2	0	$a_2 = 160$	0
$O_2 - O_3$	$-90 + \theta_3$	0	0	-90
$O_3 - O_4$	θ_4	$d_4 = 137.75$	0	90
$O_4 - O_5$	θ_5	0	0	-90
$O_5 - O_6$	0	$D_6 = 113.21$	0	0

The forward kinematics describe the transformation from one frame to another, starting at the base and ending at the end-effector. The transformation matrix A_i between two neighboring frames O_{i-1} and O_i is expressed as (1), found at the bottom of the page.

By substituting the D-H parameters in Table 1 into (1), we can obtain the individual transformation matrices A_1 to A_6 , and a global matrix of transformation 0T_6 as in (2):

$${}^0T_6 = A_1 A_2 A_3 A_4 A_5 A_6 = \begin{bmatrix} n_x & o_x & a_x & p_x \\ n_y & o_y & a_y & p_y \\ n_z & o_z & a_z & p_z \\ 0 & 0 & 0 & 1 \end{bmatrix} \quad (2)$$

where (p_x, p_y, p_z) represents the position, and $(\{n_x, n_y, n_z\}, \{o_x, o_y, o_z\}, \{a_x, a_y, a_z\})$ the orientation of the end-effector. The orientation and position of the end-effector can be calculated in terms of joint angles and the D-H parameters of the manipulator, as shown in (3) to (14).

$$n_x = c_1 s_{23} c_4 c_5 + s_1 s_4 c_5 + c_1 c_{23} s_5 \quad (3)$$

$$n_y = s_1 s_{23} c_4 c_5 - c_1 s_4 c_5 + s_1 c_{23} s_5 \quad (4)$$

$$n_z = c_{23} c_4 c_5 - s_{23} s_5 \quad (5)$$

$$A_i = Rot(z, \theta_i) Trans(0, 0, d_i) Trans(a_i, 0, 0) Rot(x, \alpha_i) = \begin{bmatrix} \cos(\theta_i) & -\sin(\theta_i) \cos(\alpha_i) & \sin(\theta_i) \sin(\alpha_i) & \alpha_i \cos(\theta_i) \\ \sin(\theta_i) & \cos(\theta_i) \cos(\alpha_i) & -\cos(\theta_i) \sin(\alpha_i) & \alpha_i \sin(\theta_i) \\ 0 & \sin(\alpha_i) & \cos(\alpha_i) & d_i \\ 0 & 0 & 0 & 1 \end{bmatrix} \quad (1)$$

$$o_x = -c_1 s_{23} s_4 + s_1 c_4 \quad (6)$$

$$o_y = -s_1 s_{23} s_4 - c_1 c_4 \quad (7)$$

$$o_z = -c_{23} s_4 \quad (8)$$

$$a_x = -c_1 s_{23} c_4 s_5 - s_1 s_4 s_5 + c_1 c_{23} c_5 \quad (9)$$

$$a_y = -s_1 s_{23} c_4 s_5 + c_1 s_4 s_5 + s_1 c_{23} c_5 \quad (10)$$

$$a_z = -c_{23} c_4 s_5 - s_{23} c_5 \quad (11)$$

$$p_x = -d_6 c_1 s_{23} c_4 s_5 - d_6 s_1 s_4 s_5 + d_6 c_1 c_{23} c_5 + d_4 c_1 c_{23} + a_2 c_1 c_2 + a_1 c_1 \quad (12)$$

$$p_y = -d_6 s_1 s_{23} c_4 s_5 + d_6 c_1 s_4 s_5 + d_6 s_1 c_{23} c_5 + d_4 s_1 c_{23} + a_2 s_1 c_2 + a_1 s_1 \quad (13)$$

$$p_z = -d_6 c_{23} c_4 s_5 - d_6 s_{23} c_5 - d_4 s_{23} - a_2 s_2 + d_1 \quad (14)$$

where $c_i = \cos(\theta_i)$, $s_i = \sin(\theta_i)$, $c_{23} = \cos(\theta_2 + \theta_3)$, and $s_{23} = \sin(\theta_2 + \theta_3)$.

3.2 Discussion of the singular position problem

It should be noted that if joint angle θ_4 equals zero, frames O_1 , O_2 , and O_4 would rotate around parallel axes, which means that all links of the arm would be on the same plane. A singular position problem^[9] might emerge in this case. This has to be checked for, before deriving the inverse kinematics. If $\theta_4 = 0$, then

$$A_4 = \begin{bmatrix} 1 & 0 & 0 & 0 \\ 0 & 0 & -1 & 0 \\ 0 & 1 & 0 & d_4 \\ 0 & 0 & 0 & 1 \end{bmatrix}, \text{ and the transforms from}$$

frame O_2 to O_5 and O_1 to O_5 , are as follows:

$${}^2T_5 = A_3 A_4 A_5 = \begin{bmatrix} s_{35} & 0 & c_{35} & c_3 d_4 \\ -c_{35} & 0 & s_{35} & s_3 d_4 \\ 0 & -1 & 0 & 0 \\ 0 & 0 & 0 & 1 \end{bmatrix} \quad (15)$$

$${}^1T_5 = A_5^2 T_5 = \begin{bmatrix} s_{235} & 0 & c_{235} & c_{23} d_4 + a_2 c_2 \\ -c_{235} & 0 & s_{235} & s_{23} d_4 + a_2 s_2 \\ 0 & -1 & 0 & 0 \\ 0 & 0 & 0 & 1 \end{bmatrix}. \quad (16)$$

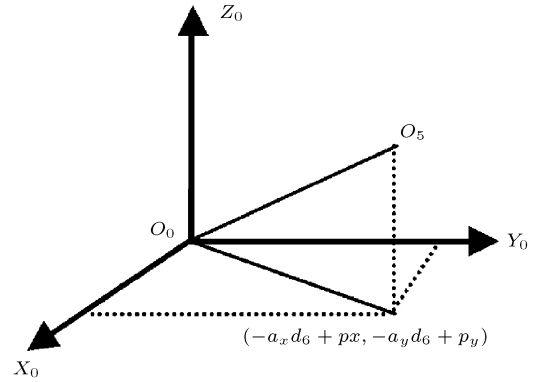
Obviously, the solutions for joint angles θ_1 to θ_5 can be determined for a given desired matrix 0T_6 . In other words, there exists no singular problem in the PArm in the case of $\theta_4 = 0$.

4 Inverse kinematics for the PArm

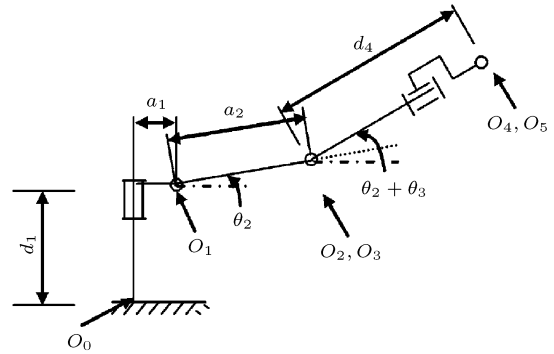
4.1 Solutions for θ_1 to θ_3

It can be observed that the origins of frames O_0 to O_5 are all in the same plane, as shown in Fig.3(b). Based on this observation, in order to simplify the

derivation of the inverse kinematics, an auxiliary frame O_5 is added, which is a rotation of the frame O_4 . The geometric projection that relates frame O_5 to frame O_1 is shown in Fig.3(a).



(a) The projection of O_5 to O_0



(b) The sketch of links in the same plane

Fig.3 The sketch of coordinate projection for the PArm

Obviously, the transformation matrix from frame O_0 to O_5 is as follows:

$${}^0T_5 = {}^0T_6 A_6^{-1} = \begin{bmatrix} n_x & o_x & a_x & -a_x d_6 + p_x \\ n_y & o_y & a_y & -a_y d_6 + p_y \\ n_z & o_z & a_z & -a_z d_6 + p_z \\ 0 & 0 & 0 & 1 \end{bmatrix} \quad (17)$$

and from Fig.3(a) it is easy to find a solution for θ_1 as follows:

$$\begin{cases} \theta_{11} = \arctan 2(-a_y d_6 + p_y, -a_x d_6 + p_x) \\ \theta_{12} = \arctan 2(a_y d_6 - p_y, a_x d_6 - p_x) \end{cases} \quad (18)$$

where θ_{11} and θ_{12} are two candidate solutions, which correspond to the front and rear arm locations.

From Fig.3(b), considering the direction of angles

θ_2 and θ_3 , we have:

$$\begin{cases} d_1 - a_2 s_2 - d_4 s_{23} = -a_z d_6 + p_z \\ a_1 + a_2 c_2 + d_4 c_{23} = \\ \pm \sqrt{(-a_x d_6 + p_x)^2 + (-a_y d_6 + p_y)^2} \end{cases} \quad (19)$$

where the positive sign on the right hand side of the second equation is for the front arm orientation, and the negative sign for the rear arm orientation. In other words, the positive corresponds to θ_{11} and the negative to θ_{12} . For the sake of convenience, (19) is rewritten as (20):

$$\begin{cases} d_4 s_{23} = a_z d_6 - p_z + d_1 - a_2 s_2 = B_1 - a_2 s_2 \\ d_4 c_{23} = \pm \sqrt{(-a_x d_6 + p_x)^2 + (-a_y d_6 + p_y)^2} \\ -a_1 - a_2 c_2 \\ = B_2 - a_2 c_2 \end{cases} \quad (20)$$

where

$$\begin{cases} B_1 = a_z d_6 - p_z + d_1 \\ B_2 = \pm \sqrt{(-a_x d_6 + p_x)^2 + (-a_y d_6 + p_y)^2} - a_1 \end{cases} \quad (21)$$

By applying a square sum to the two equations in (20), a new equation that contains θ_2 alone can be formed as follows:

$$B_1 s_2 + B_2 c_2 = \frac{B_1^2 + B_2^2 + a_2^2 - d_4^2}{2a_2} \quad (22)$$

It is easy to establish that the values of B_1 and B_2 are not zero at the same time. Otherwise (22) would not hold because of the different values of a_2 and d_4 . Therefore, it is reasonable to introduce an auxiliary angle γ which is defined by:

$$\gamma = \arctan 2(B_2, B_1). \quad (23)$$

By combining (23) and (22), a solution for θ_2 can be derived as follows:

$$\begin{cases} \theta_{21} = \arcsin\left(\frac{B_1^2 + B_2^2 + a_2^2 - d_4^2}{2a_2\sqrt{B_1^2 + B_2^2}}\right) - \gamma \\ \theta_{22} = \pi - \arcsin\left(\frac{B_1^2 + B_2^2 + a_2^2 - d_4^2}{2a_2\sqrt{B_1^2 + B_2^2}}\right) - \gamma \end{cases} \quad (24)$$

where θ_{21} and θ_{22} are two candidate values for θ_2 . From (20), we can obtain a solution for θ_3 :

$$\theta_3 = \arctan 2(B_1 - a_2 s_2, B_2 - a_2 c_2) - \theta_2. \quad (25)$$

It is clear that there are four groups of possible solutions for θ_1 , θ_2 , and θ_3 .

4.2 Solutions for θ_4 and θ_5

After obtaining solutions for θ_1 , θ_2 , and θ_3 , it should be straightforward to obtain solutions for θ_4 and θ_5 by using the equations for the forward kinematics^[2]. However, various conditions with different values for solved joint angles have to be considered. This paper proposes a useful strategy to solve θ_4 and θ_5 , and at the same time obtain useful criteria for checking the correctness of solutions. From (2), we have:

$$A_3^{-1} A_2^{-1} A_1^{-1} {}^0 T_6 A_6^{-1} = A_4 A_5 \quad (26)$$

where the right side is:

$$A_4 A_5 = \begin{bmatrix} c_4 c_5 & -s_4 & -c_4 s_5 & 0 \\ s_4 c_5 & c_4 & -s_4 s_5 & 0 \\ s_5 & 0 & c_5 & d_4 \\ 0 & 0 & 0 & 1 \end{bmatrix} \quad (27)$$

and the left side is easily derived as (28). By substituting s_1 , c_1 , s_{23} , and c_{23} obtained from (18), (24), and (25) into the last column in (28), we have (29).

$$A_3^{-1} A_2^{-1} A_1^{-1} {}^0 T_6 A_6^{-1} = \begin{bmatrix} n_x c_1 s_{23} + n_y s_1 s_{23} + n_z c_{23} & o_x c_1 s_{23} + o_y s_1 s_{23} + o_z c_{23} & a_x c_1 s_{23} + a_y s_1 s_{23} + a_z c_{23} \\ n_x s_1 - n_y c_1 & o_x s_1 - o_y c_1 & a_x s_1 - a_y c_1 \\ n_x c_1 c_{23} + n_y s_1 c_{23} - n_z s_{23} & o_x c_1 c_{23} + o_y s_1 c_{23} - o_z c_{23} & a_x c_1 c_{23} + a_y s_1 c_{23} - a_z s_{23} \\ 0 & 0 & 0 \end{bmatrix} \begin{bmatrix} c_1 s_{23}(-a_x d_6 + p_x) + s_1 s_{23}(-a_y d_6 + p_y) + c_{23}(-a_z d_6 + p_z) - a_1 s_{23} - a_2 s_3 - d_1 c_{23} \\ s_1(-a_x d_6 + p_x) - c_1(-a_y d_6 + p_y) \\ c_1 c_{23}(-a_x d_6 + p_x) + s_1 c_{23}(-a_y d_6 + p_y) + s_{23}(-a_z d_6 + p_z) - a_1 c_{23} - a_2 c_3 - d_1 s_{23} \\ 1 \end{bmatrix} \quad (28)$$

$$A_3^{-1} A_2^{-1} A_1^{-1} {}^0 T_6 A_6^{-1} = \begin{bmatrix} n_x c_1 s_{23} + n_y s_1 s_{23} + n_z c_{23} & o_x c_1 s_{23} + o_y s_1 s_{23} + o_z c_{23} & a_x c_1 s_{23} + a_y s_1 s_{23} + a_z c_{23} & 0 \\ n_x s_1 - n_y c_1 & o_x s_1 - o_y c_1 & a_x s_1 - a_y c_1 & 0 \\ n_x c_1 s_{23} + n_y s_1 s_{23} - n_z c_{23} & o_x c_1 s_{23} + o_y s_1 s_{23} - o_z c_{23} & a_x c_1 s_{23} + a_y s_1 s_{23} - a_z c_{23} & d_4 \\ 0 & 0 & 0 & 1 \end{bmatrix} \quad (29)$$

By equating the first and second terms of the second column in (27) and (29) respectively, we can obtain a solution for θ_4 . Similarly, by equating the first and third terms of the third row in (27) and (29) respectively, we can obtain a solution for θ_5 . The solutions for θ_4 and θ_5 are as follows:

$$\begin{cases} \theta_4 = \arctan 2(-o_x c_1 s_{23} - o_y s_1 s_{23} - o_z c_{23}, o_x s_1 o_y c_1) \\ \theta_5 = \arctan 2(n_x c_1 c_{23} + n_y s_1 c_{23} - n_z s_{23} - a_x c_1 c_{23} \\ \quad + a_y s_1 s_{23} - a_z s_{23}). \end{cases} \quad (30)$$

4.3 The existence of correct solutions

It is evident that the inverse kinematics for a 5-DOF manipulator such as the PArm will have no solution for some given positions and orientations of the end-effector. How can we know in which cases there will be no solution to the inverse kinematics? We notice that the term in the third row and second column in (27) is zero and the corresponding term in (29) is determined by θ_1 to θ_3 , so that we have the following criterion—the solutions for θ_1 , θ_2 , and θ_3 have to satisfy:

$$o_x c_1 c_{23} + o_y s_1 c_{23} - o_z s_{23} = 0. \quad (31)$$

The physical meaning of this criterion can easily be explained. As a matter of fact, $[c_1 c_{23} \ s_1 c_{23} \ -s_{23}]^T$ is the direction vector of the Z-axis of frame O_3 , whilst $[o_x \ o_y \ o_z]^T$ is that of the Y-axis of frame O_5 . As shown in Fig.1, these two axes have perpendicular mechanics at any given time. Therefore, the relationship expressed in (31) can be used in the following two criteria for checking whether there are feasible inverse kinematic solutions.

Criterion 1: The inverse kinematics for the PArm have correct solutions, if and only if at least one of the solutions for θ_1 to θ_3 , given in (18), (24), and (25), satisfies (31).

Proof.

a) The necessity

If (31) is not satisfied by any of the four groups of solutions given in (18), (24), and (25), then (26) cannot be satisfied and the position and orientation of the end-effector cannot be achieved with these solutions.

b) The sufficiency

If (31) is satisfied by any of the four groups of solutions given in (18), (24), and (25), then the solutions for θ_4 and θ_5 given by (30) will satisfy (26), because of the orthogonality of the rotation transformation matrix for the orientation. That is, the desired position and orientation of the end-effector can be realized. \square

There are four groups of candidate solutions given above. Although the above criterion can be employed

to check how many of those groups belong to correct solutions, an easier way is to predict the number of correct solutions in terms of the desired position and orientation of the end-effector. The direction vector of the Z-axis of frame O_3 can be indicated using different candidate solutions for θ_1 and θ_2 as follows:

$$\begin{cases} v_{z31} = [c_1 c_{231} \ s_1 c_{231} \ -s_{231}]^T, \text{ for } \theta_{11}, \theta_{21}, \theta_{231} \\ v_{z32} = [c_1 c_{232} \ s_1 c_{232} \ -s_{232}]^T, \text{ for } \theta_{11}, \theta_{22}, \theta_{232} \\ v_{z33} = [-c_1 c_{233} \ -s_1 c_{233} \ -s_{233}]^T, \text{ for } \theta_{12}, \theta_{21}, \theta_{233} \\ v_{z34} = [-c_1 c_{234} \ -s_1 c_{234} \ -s_{234}]^T, \text{ for } \theta_{12}, \theta_{22}, \theta_{234} \end{cases} \quad (32)$$

where v_{z31} to v_{z34} represent the direction of the Z-axis of frame O_3 in frame O_0 .

Any two vectors in (32) form a plane because of the different values of θ_{231} to θ_{234} . For example, v_{z3i} and v_{z3j} ($i \neq j$) form a plane with a vertical vector as:

$$v_{3ij} = v_{z3i} \times v_{z3j} = [-s_1 k_{ij} \ c_1 k_{ij} \ 0]^T \quad (33)$$

where $k_{ij} = c_{23i} s_{23j} - s_{23i} c_{23j}$. It is clear that $k_{ij} \neq 0$ for $\theta_{23i} \neq \theta_{23j}$ when $i \neq j$. The cross product of the Y-axis of frame O_5 and v_{3ij} is given by:

$$v_{3ij} \times v_{y5} = [k_{ij} o_z c_1 \ k_{ij} o_z s_1 \ -k_{ij}(o_x c_1 + o_y s_1)]^T \quad (34)$$

where $v_{y5} = [o_x \ o_y \ o_z]^T$ is the Y-axis of frame O_5 . If $v_{3ij} \times v_{y5} = [0 \ 0 \ 0]^T$, then the Y-axis of frame O_5 is vertical to the plane formed with v_{z3i} and v_{z3j} . This means that the solutions corresponding to v_{z3i} and v_{z3j} are correct because they satisfy (31). This observation leads to the following criterion.

Criterion 2: Multiple groups of correct solutions exist if and only if (35) and (36) are satisfied:

$$\begin{cases} o_x(p_x - a_x d_6) + o_y(p_y - a_y d_6) = 0 \\ o_z = 0 \end{cases} \quad (35)$$

$$(a_2 - d_4)^2 \leq B_1^2 + B_2^2 \leq (a_2 + d_4)^2. \quad (36)$$

Condition (35) is derived from (34) and (31) under the condition that s_1 and c_1 are not zero at the same time. To ensure that the solutions for θ_1 to θ_3 given in (18), (24), and (25) have real values, condition (36) must be satisfied. If conditions (35) and (36) are satisfied, there will be two or four solution groups that can achieve the desired position and orientation of the end-effector. More specifically, the following conclusions can be drawn:

- In the case that (35) and (36) are satisfied for two selections of B_2 , four groups of correct solutions can be obtained.
- If (35) is satisfied, but (36) is true for only one selection of B_2 , then two groups of correct solutions can be obtained.

- If (35) is satisfied, but (36) is false for two selections of B_2 , there will be no correct solutions, because of the mechanical constraints.
- If (35) is not satisfied, but (31) is satisfied, there will be a unique group of solutions to realize the desired position and orientation of the end-effector.
- If (35) and (31) are not satisfied, there will be no solution to realize the desired position and orientation of the end-effector.

It is noted that when (35) is satisfied then $\theta_4 = 0$ or $\theta_4 = \pm\pi$. This means that all links and the end-effector in this case are in the same plane, and that the conclusion in Section 3.2 is supported.

5 Inverse kinematics for the PARM with one DOF of the end-effector unsatisfied

5.1 Solutions that satisfy the position and Z-axis orientation

As discussed in Section 1, the position of the end-effector has to be controlled accurately, but only the desired Z-axis orientation should be matched in some applications, i.e. the X or Y-axis orientation is ignored. In this case, the solutions for θ_1 to θ_3 are the same as given in Section 4.1, because they are able to realize the desired position of the end-effector.

To take only the Z-axis orientation into account, the terms in the third row and third column in (27) and (29) are used to obtain a solution for θ_5 as follows:

$$\theta_5 = \pm \arccos(a_x c_1 c_{23} + a_y s_1 c_{23} - a_z s_{23}). \quad (37)$$

Then, the first and second terms in the third column in (27) and (29) can be used to solve θ_4 . Here three cases are presented:

- If $s_5 > 0$ then the solution for θ_4 is:

$$\theta_{41} = \arctan 2(-a_x s_1 + a_y c_1, -a_x c_1 s_{23} - a_y s_1 s_{23} - a_z c_{23}) \quad (38)$$

- If $s_5 < 0$ then the solution for θ_4 is:

$$\theta_{42} = \arctan 2(a_x s_1 - a_y c_1, a_x c_1 s_{23} + a_y s_1 s_{23} + a_z c_{23}) \quad (39)$$

- If $s_5 = 0$, then a_x and a_y are independent of θ_4 , which can be checked in (9) and (10). Therefore, the solution of θ_4 can be given arbitrarily in this case.

5.2 Solutions to satisfy all orientations

Now consider the situation where all orientations can be satisfied and the position coordinates in the Y and Z axes are also taken into account. For example, if the manipulator is installed on a mobile robot, then the position coordinate on the X-axis could be realized by the mobile robot.

It can be noted that the first term is the product of the second and third terms in (27). Therefore, an equation including only θ_1 to θ_3 can be formed as follows:

$$\begin{aligned} n_x c_1 s_{23} + n_y s_1 s_{23} + n_z c_{23} \\ = (o_x s_1 - o_y c_1)(a_x c_1 c_{23} + a_y s_1 c_{23} - a_z s_{23}). \end{aligned} \quad (40)$$

Another equation including only θ_1 to θ_3 is (31). If $o_z \neq 0$ then s_{23} can be expressed using c_{23} , s_1 , and c_1 . Combining (31) and (40) leads to:

$$\begin{aligned} n_y o_y (o_z - 1) + (n_x o_x - n_y o_y)(o_z - 1)c_1^2 \\ + (n_x o_y + n_y o_x)(o_z - 1)c_1 s_1 = 0. \end{aligned} \quad (41)$$

If $o_z \neq 1$, then the common term $o_z - 1$ can be eliminated from (41). By applying a double angle formula to (41), a typical triangle equation can be obtained as follows:

$$(n_x o_x - n_y o_y) \cos(2\theta_1) + (n_x o_y + n_y o_x) \sin(2\theta_1) = n_z o_z \quad (42)$$

and possible solutions for θ_1 derived as:

$$\begin{cases} \gamma_1 = \arctan 2(n_x o_x - n_y o_y, n_x o_y + n_y o_x) \\ \gamma_2 = \arcsin \frac{n_z o_z}{\sqrt{(1 - n_z^2)(1 - o_z^2)}} \\ \theta_{11} = (\gamma_2 - \gamma_1)/2 \\ \theta_{12} = (\pi - \gamma_2 - \gamma_1)/2 \\ \theta_{13} = \pi + (\gamma_2 - \gamma_1)/2 \\ \theta_{14} = \pi + (\pi - \gamma_2 - \gamma_1)/2 \end{cases} \quad (43)$$

where γ_1 and γ_2 are auxiliary angles, and θ_{11} to θ_{14} are four candidate solutions for θ_1 .

By substituting θ_1 in (31) using (43), the value of θ_{23} can then be determined as follows:

$$\begin{cases} \theta_{231} = \arctan 2(o_x c_1 + o_y s_1, -o_z) \\ \theta_{232} = \pi + \theta_{231} \end{cases} \quad (44)$$

where θ_{231} and θ_{232} are two candidate solutions for θ_{23} .

The position coordinates on the axes X, Y, and Z of frame O_6 in the base frame show the relationship between θ_1 to θ_3 as in (45):

$$\begin{cases} d_1 - a_2 s_2 - d_4 s_{23} = -a_z d_6 + p_z \\ (a_1 + a_2 c_2 + d_4 c_{23}) s_1 = -a_y d_6 + p_y \\ (a_1 + a_2 c_2 + d_4 c_{23}) c_1 = -a_x d_6 + p_x \end{cases} \quad (45)$$

By submitting θ_{23} to the first equation in (45), then solutions for θ_2 and θ_3 can be obtained as (46) and (47):

$$\begin{cases} \theta_{21} = \arcsin[(d_1 - d_4 s_{23} + a_z d_6 - p_z)/a_2] \\ \theta_{22} = \pi - \theta_{21} \end{cases} \quad (46)$$

where θ_{21} and θ_{22} are two candidate solutions for θ_2 , and the solution for θ_3 is:

$$\theta_3 = \theta_{23} - \theta_2. \quad (47)$$

The solutions for θ_4 and θ_5 can be given as in (30). In this case, the reachable positions p_x and p_y can be calculated from the last two equations in (45), which may be far away from the desired positions.

If $o_z = 1$, then $o_x = 0$ and $o_y = 0$. The result $\theta_{23} = 0$ can be deduced from (31). By submitting θ_{23} in (45), the solutions for θ_1 to θ_3 can be obtained as in (48) and (49):

$$\begin{cases} \theta_{21} = \arcsin[(d_1 + a_z d_6 - p_y)/a_2] \\ \theta_{22} = \pi - \theta_{21} \\ \theta_3 = -\theta_2 \end{cases} \quad (48)$$

$$\begin{cases} \gamma_4 = \arcsin[(-a_y d_6 + p_y)/(a_1 + a_2 c_2 + d_4 c_{23})] \\ \theta_{11} = \gamma_4 \\ \theta_{12} = \pi - \gamma_4 \end{cases} \quad (49)$$

where θ_{11} and θ_{12} are two candidate solutions for θ_1 .

If $o_z = 0$, then $c_{23} = 0$ or $s_4 = 0$. If $c_{23} = 0$, then the solution of θ_1 to θ_3 can be obtained from (45). If $s_4 = 0$, θ_1 can be resolved from (31), and θ_2 and θ_3 deduced from (45). The solution of θ_4 and θ_5 can be given as (30). The processes of resolution in detail for these cases are omitted here.

Obviously, even if positions in the X and Y axes are not considered, it is not certain that the orientation of the end-effector can be realized, because $d_1 - d_4 s_{23} + a_z d_6 - p_z$ may be greater than a_2 . Therefore, solutions to satisfy the orientation of the end-effector first are not considered.

6 Experimental results

Several experiments were conducted to validate the derived inverse kinematics. An experiment was first conducted to check the correctness of the method derived in Section 4, with reachable positions and orientations. The desired positions and orientations of the end-effector were created using forward kinematics with random joint angles^[10]. Therefore, these positions and orientations were reachable by the manipulator. Experiment results show that the derived inverse kinematics provide completely accurate solutions in this experiment. In addition, criteria 1 and 2 described by (31), (35), and (36) are also proved correct.

6.1 Experiment of trajectory following

In this experiment, desired positions and orientations of the end-effector were generated using:

$${}^0T_6 = \begin{bmatrix} 1 & 0 & 0 & p_x \\ 0 & -1 & 0 & p_y \\ 0 & 0 & -1 & p_z \\ 0 & 0 & 0 & 1 \end{bmatrix} \quad (50)$$

$$\begin{cases} p_x = 298 + t/5 \\ p_y = 50 \cos(\pi t/36) \\ p_z = 100 - 40 \sin(\pi t/36) \end{cases} \quad (51)$$

where $t(= 1, 2, \dots, 36)$ is an independent variable. The orientations were fixed, and the positions formed a smooth trajectory. Obviously, there were unreachable positions. This experiment was conducted to test solutions derived in both Sections 4 and 5.1.

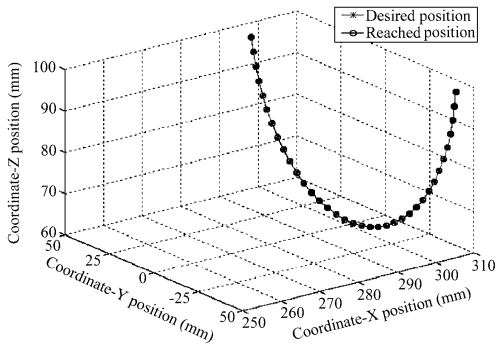
The methods proposed in Sections 4 and 5.1 were employed to find joint angles from the desired positions and orientations. Then, the forward kinematics were applied to calculate the reached positions and orientations. The angles formed by the inverse kinematics were applied to the PArm manipulator in a real robot experiment. Both the simulated PArm and the real PArm were used in experiments. Joint angle accuracy for the simulated PArm and real PArm were 0.01 and 1 degree respectively.

Experiment results for the simulated PArm are given in Fig. 4, and those for the real PArm in Fig. 5. Figs. 4(a) and 5(a) show desired positions with stars, and reached positions with circles. Coordinate units are in millimeters. Figs. 4(b) and 5(b) show orientation errors in terms of Euler angles. Figs. 4(c) and 5(c) illustrate orientation errors in terms of angles between desired and reached axis directions. Figs. 4(d) and 5(d) display joint angles from the inverse kinematics.

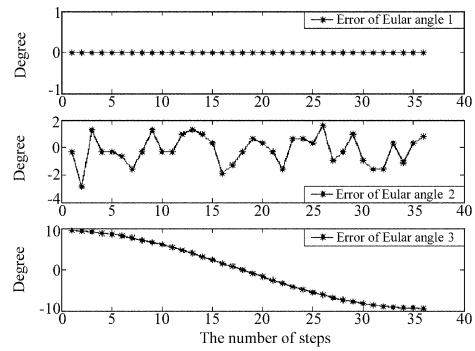
From Figs. 4 and 5 it is clear that all desired positions match with mm accuracy and the Z -axis orientation is well satisfied. However, this is not the case with the X and Y -axis orientations, because the methods applied here satisfy the positions and the Z -axis orientation without considering the remained DOF in orientation.

6.2 Experiment for unreachable positions and orientations near reachable ones

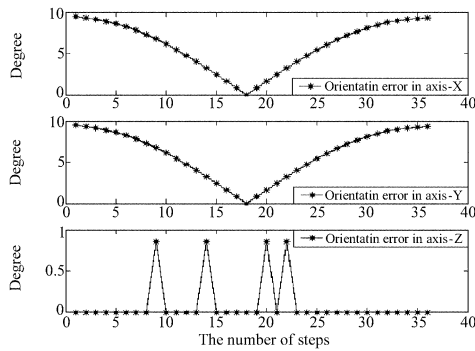
This simulation experiment was used to check if a group of reasonable solutions could be obtained for positions and orientations near reachable ones. Reachable positions and orientations were generated using the forward kinematics with random joint angles, as conducted in experiment 1. Their Euler angles indica-



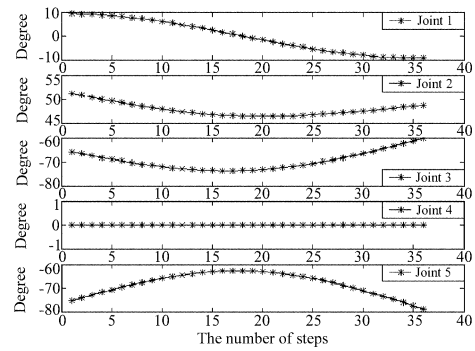
(a) Desired and reached positions



(b) Orientation errors in terms of Euler angles

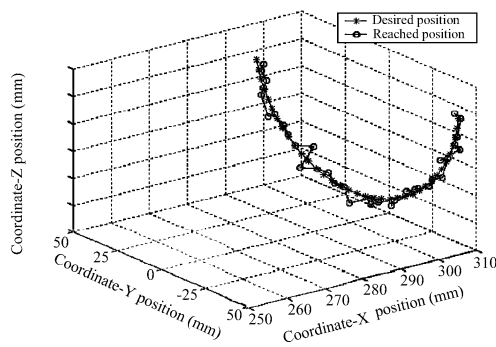


(c) Orientation errors in terms of angles between desired and reached axis directions

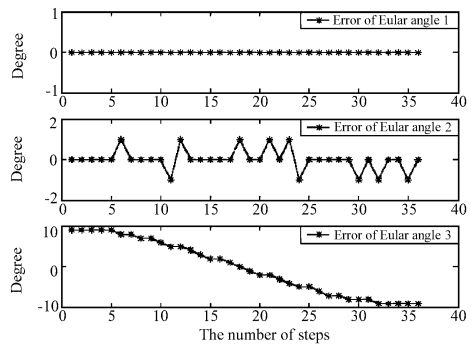


(d) Joint angles

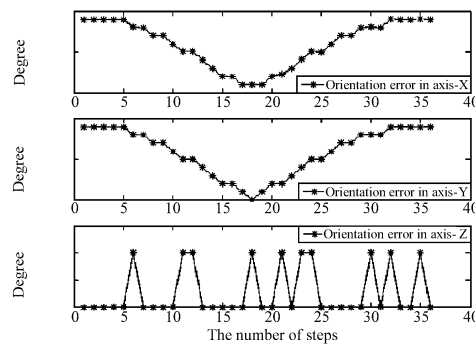
Fig.4 Experimental results using the simulated PARM



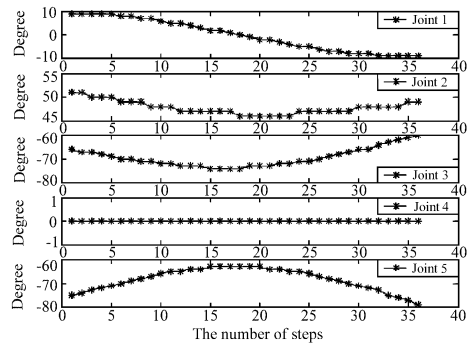
(a) Desired and reached positions



(b) Orientation errors in terms of Euler angles



(c) Orientation errors in terms of angles between desired and reached axis directions



(d) Joint angles

Fig.5 Experimental results using the real PARM

ting orientations were calculated, and then added using small random angles in the range $[-1.5 \ 1.5]$ degrees. Positions were also added using random values, ranging between $[-2 \ 2]$ mm. In this way, positions and orientations in a small neighborhood of reachable ones were generated. The values of joint angles were strictly limited in their actual working range, and their accuracy set the same as for the real PArm, i.e. one degree. When values of solutions exceeded this range, a simple optimal search method using a grade-descent strategy was employed to find a group of approximate solutions in the range. It used the calculated solutions as initial starting points. It is clear that a group of satisfied approximate solutions can be found for any unreachable positions and orientations near reachable ones by using the inverse kinematics calculation combined with the grade-descent searching strategy. Inverse kinematics results are shown in Fig.6 for positions, and Fig.7 for errors of positions and the Z-axis orientation, respectively. It can be concluded that the three-dimensional positions and the Z-axis orientation can be effectively

satisfied, whether the orientation of the end-effector is reachable or not.

6.3 A comparison of methods described in Section 5

The last experiment compared the methods derived in Sections 5.1 and 5.2 with unreachable positions and orientations of the end-effector. Experiment results are provided below as T_d , T_1 , and T_2 , where T_d is the desired unreachable position and orientation, T_1 is the reached position and orientation obtained by using the method in Section 5.1, and T_2 is the reached position and orientation obtained by using the method in Section 5.2. It can be seen that the position and Z-axis orientation in T_1 match T_d very well and the remaining orientation is close to that in T_d . The orientations in T_2 are almost the same as those in T_d , but the positions are far from those in T_d . Therefore, the method in Section 5.1 provides advantages in comparison to the method in Section 5.2.

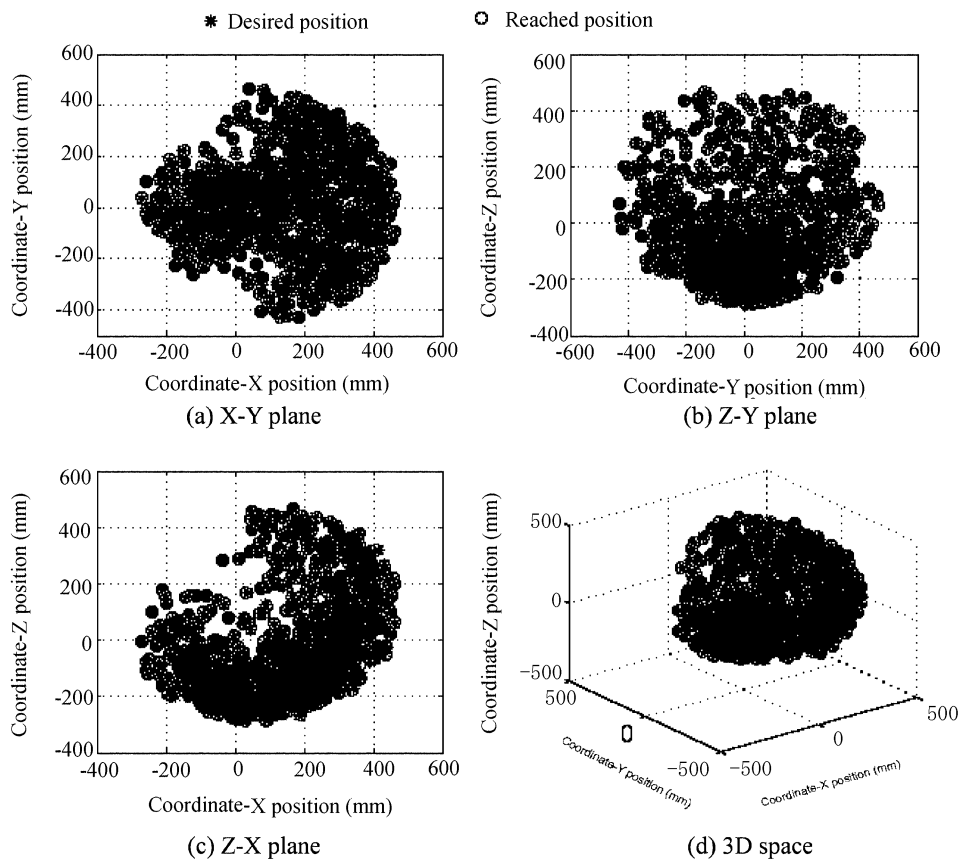


Fig.6 Desired and reached positions on planes and in 3D space

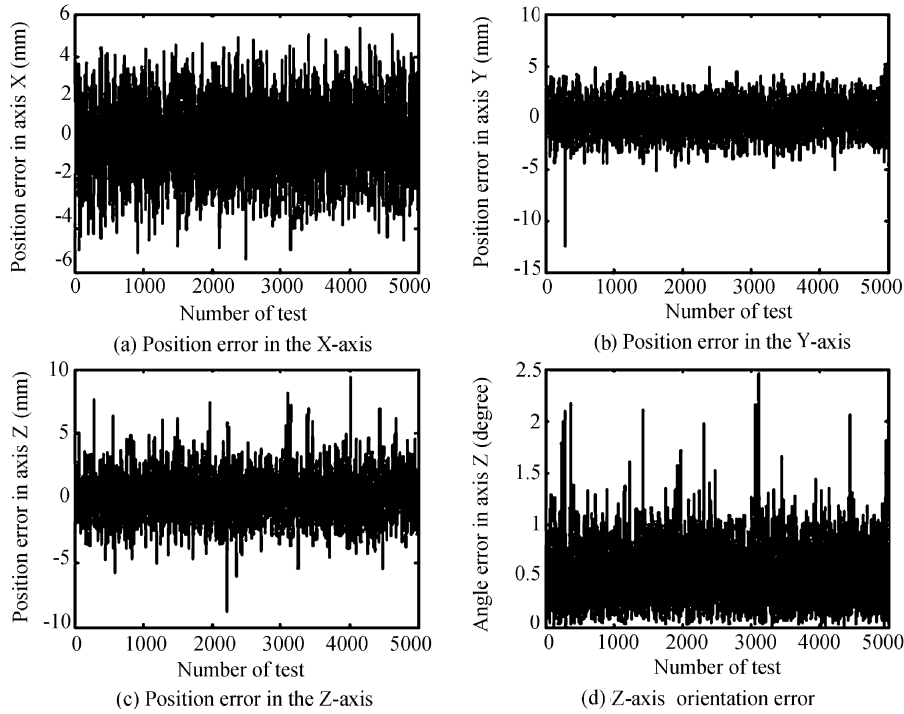


Fig.7 Error in positions and in Z-axis orientation

$$T_d = \begin{bmatrix} 0.0630 & 0.3871 & 0.9199 & 262.3470 \\ -0.8761 & 0.4629 & -0.1348 & 279.1224 \\ -0.4780 & -0.7974 & 0.3683 & 286.1055 \\ 0 & 0 & 0 & 1 \end{bmatrix}$$

$$T_1 = \begin{bmatrix} 0.0587 & 0.3878 & 0.9199 & 262.3453 \\ -0.8812 & 0.4531 & -0.1348 & 279.1235 \\ -0.4691 & -0.8027 & 0.3683 & 286.1053 \\ 0 & 0 & 0 & 1 \end{bmatrix}$$

$$T_2 = \begin{bmatrix} 0.0630 & 0.3871 & 0.9199 & 198.9438 \\ -0.8761 & 0.4629 & -0.1348 & 161.1466 \\ -0.4780 & -0.7974 & 0.3683 & 266.6803 \\ 0 & 0 & 0 & 1 \end{bmatrix}.$$

7 Conclusions and future work

In this paper, a strategy based on geometric projection was proposed to resolve the inverse kinematics of a 5-DOF manipulator. Sufficient and necessary criteria were provided to determine whether correct solutions existed without using forward kinematics. Once the four groups of candidate solutions were calculated for the first three joint angles, one criterion was employed to check which group was correct. In addition, it was possible using another criterion to check if there were multiple groups of correct solutions for a given position and orientation before resolving the inverse kinematics. Both criteria were derived for the first time in this paper. They provide significant convenience for the

resolving process of inverse kinematics. This is an important advancement, since the singular problem often exists in 6-DOF manipulators.

The effectiveness of the derived methods has been demonstrated through experiment results. For any reachable positions and orientations of the end-effector, correct solutions for the inverse kinematics of the PArm could be obtained from (18), (21), (23), (24), (25), and (30). Their correctness can be checked using criterion (31). For dealing with unreachable positions and orientations of an end-effector, solutions that satisfy the positions and the Z-axis orientation are preferred and can be used to satisfy applications such as those in [11] and [12]. We have currently focused on the problem associated with a mobile manipulator, i.e. a combination of a manipulator and a mobile robot. Although the manipulator has insufficient DOF, the addition of a 3-DOF mobile platform makes its DOF redundant; this in turn creates new problems for us to address in the future.

References

- [1] D. Manocha, J. F. Canny. Efficient inverse kinematics for general 6R manipulators. *IEEE Transactions on Robotics and Automation*, vol. 10, no. 5, pp. 648–657, 1994.
- [2] J. Q. Gan, E. Oyama, E. M. Rosales, H. Hu. A complete analytical solution to the inverse kinematics of the Pioneer2 robotic arm. *Journal of Robotica*, vol. 23, no. 1, pp. 123–129, 2005.
- [3] J. Guo, V. Cherkassky. A solution to the inverse kinemat-

ics problem in robotics using neural network processing. *In proceedings of IEEE Conference on Neural Networks*, Washington, D.C., USA, pp. 299-304, 1989.

- [4] S. Tejomurtula, S. Kak. Inverse kinematics in robotics using neural networks. *Information Sciences*, vol. 116, pp. 147-164, 1999.
- [5] E. Oyama, A. Agah, K. F. MacDprman, S. Tachi. A modular neural network architecture for inverse kinematics model learning. *Neuro-computing*, vol. 38-40, pp. 797-805, 2001.
- [6] E. Papadopoulos, J. Poulakakis. Planning and model-based control for mobile manipulators. *In proceedings of IEEE/RSJ International Conference on Intelligent Robots and Systems*, Takamatsu, Japan, 1810-1815, 2000.
- [7] C. S. Tzafestas, S. G. Tzafestas. Full-state modelling, motion planning and control of mobile manipulators. *Studies in Informatics and Control*, vol.10, no.2, 2001. [Online], Available: http://www.ici.ro/ici/revista/sic2001_2/index.html
- [8] ActivMedia Robotics' Pioneer Arm Manual v4, September, 2003. ActivMedia
- [9] D. Xu. A study on visual measurement and control for robot. *Post-Doctoral Fellow Report*, chapter 2, Institute of Automation, China, 2002.
- [10] E. M. Rosales, J. Q. Gan. Forward and inverse kinematics models for a 5-DOF pioneer 2 robot arm. *Technical report*, University of Essex, 2003.
- [11] L. Zlajpah, B. Nemeč. Kinematic control algorithms for on-line obstacle avoidance for redundant manipulators. *IEEE/RSJ International Conference on Intelligent Robots and Systems*, Lausanne, Switzerland, 1898-1903, 2002.
- [12] M. A. Meggiolaro, G. Scriffignano, S. Dubowsky. Manipulator calibration using a single endpoint contact constraint. *In Proceedings of ASME Design Engineering Technical Conference*, Baltimore, USA, 2000.



De Xu graduated from Shandong University of Technology (SUT), China in 1985. He received a Masters degree from SUT in 1990, and a Ph.D. degree from Zhejiang University, China in 2001. He has been with the Institute of Automation, at the Chinese Academy of Sciences (CASIA) since 2001. He is an associate professor with the Laboratory of Complex Systems and Intelligence Science, CASIA. He

worked as on academic visitor in the Department of Computer Science, at the University of Essex from May to August 2004. He is a member of the IEEE. His research interests include robotics and automation, especially the control of robots such as visual and intelligent control.



Carlos Antonio Acosta Calderon received a B.S. degree in Computer Science Engineering from Pachuca Institute of Technology, Mexico in 2000, and a M.Sc. degree in Computer Science (Robotics and Intelligent Machines) from the University of Essex, UK in 2001. He is currently pursuing a Ph.D degree in Computer Science at the University of Essex, UK. His research interests have focused on

mobile robots, in particular, the coordination of multi-robot systems, mobile manipulators, and learning by imitation. He is a member of IEEE.



John Q. Gan received a B.Sc. degree in electronic engineering from Northwestern Polytechnic University, China in 1982, a M.Eng. degree in automatic control and a Ph.D degree in biomedical electronics from Southeast University, China in 1985 and 1991, respectively. He is a Senior Lecturer in the Department of Computer Science at the University of Essex, UK. He has

co-authored a book, and published over 100 research papers. His research interests are in robotics and intelligent systems, brain-computer interfaces, pattern recognition, signal processing, data fusion, and neurofuzzy computation.



Huosheng Hu is a Professor in the Department of Computer Science, at the University of Essex, and head of the Human Centered Robotics Group. His research interests include autonomous mobile robots, human-robot interaction, evolutionary robotics, multi-robot collaboration, embedded systems, pervasive computing, sensor integration, RoboCup, intelligent control, and networked robotics. He has published over 200 papers in journals, books, and conferences, and received two best paper awards. He is a founding member of the IEEE Society of Robotics and Automation Technical Committee of Internet and Online Robots, and a member of the IASTED Technical Committee on "Robotics" for 2001-2004. He was a Conference Chairman for the 1st European Embedded Systems Conference in Paris, 1996, and has been a member of the Program Committees for many international conferences such as IROS (2005-2006), IASTED Robotics and Applications Conferences (2000-present), and RoboCup Symposiums (2000 - 2004). Dr. Hu is a Chartered Engineer, a senior member of IEEE, and a member of IEE, AAAI, ACM, IASTED and IAS.

He has published over 200 papers in journals, books, and conferences, and received two best paper awards. He is a founding member of the IEEE Society of Robotics and Automation Technical Committee of Internet and Online Robots, and a member of the IASTED Technical Committee on "Robotics" for 2001-2004. He was a Conference Chairman for the 1st European Embedded Systems Conference in Paris, 1996, and has been a member of the Program Committees for many international conferences such as IROS (2005-2006), IASTED Robotics and Applications Conferences (2000-present), and RoboCup Symposiums (2000 - 2004). Dr. Hu is a Chartered Engineer, a senior member of IEEE, and a member of IEE, AAAI, ACM, IASTED and IAS.



Min Tan graduated from Tsing Hua University, China in 1986. He received a Ph.D. degree in 1990 from CASIA. He is a professor with the Laboratory of Complex Systems and Intelligence Science, CASIA. He has published over 100 papers in journals, books, and conferences. His research interests include robotics and complex system theory.